

## Title Page

# TITLE: DERIVATIVES OF PIPERAZINES AS POTENTIAL THERAPEUTIC AGENTS FOR ALZHEIMER'S DISEASE

**Elena Popugaeva<sup>1</sup>, Daria Chernyuk<sup>1</sup>, Hua Zhang<sup>2</sup>, Tatyana Y. Postnikova<sup>3</sup>,  
Karina Pats<sup>4</sup>, Elena Fedorova<sup>4</sup>, Vladimir Poroikov<sup>5</sup>, Aleksey V. Zaitsev<sup>3,6</sup>, Ilya  
Bezprozvanny<sup>1,2,§</sup>**

§Corresponding author

<sup>1</sup>Laboratory of Molecular Neurodegeneration, Department of Medical Physics, Peter the Great St. Petersburg Polytechnic University, St. Petersburg, Russian Federation, 195251; <sup>2</sup>Department of Physiology, UT Southwestern Medical Center at Dallas, Dallas, TX, USA, 75390; <sup>3</sup>Laboratory of Molecular Mechanisms of Neural Interactions, Sechenov Institute of Evolutionary Physiology and Biochemistry of the Russian Academy of Sciences, Saint Petersburg, Russian Federation, 194223; <sup>4</sup>VVS Lab Inc., Ulica Dostoevskogo 44, Saint Petersburg, Russian Federation, 191119; <sup>5</sup> Institute of Biomedical Chemistry, 10/8 Pogodinskaya St., Moscow, Russian Federation, 119121; <sup>6</sup>Institute of Experimental Medicine, Almazov National Medical Research Centre, St. Petersburg, Russian Federation, 197341

## Running Title Page

### Running Title: Piperazines as potential neuroprotective agents

§Corresponding author: Dr. Ilya Bezprozvanny

Address: 5323 Harry Hines Boulevard, ND12.200A, Dallas, TX 75390

Phone: 214-645-6017

Fax: 214-645-6018

E-mail: [Ilya.Bezprozvanny@UTSouthwestern.edu](mailto:Ilya.Bezprozvanny@UTSouthwestern.edu)

Number of text pages: 37

Number of Tables: 2

Number of Figures: 7

Number of References: 31

Number of words in Abstract: 224 (must not exceed 250)

Number of words in Introduction: 740 (must not exceed 750)

Number of words in Discussion: 916 (must not exceed 1500)

#### List of abbreviations:

a.u. – arbitrary unit

AD – Alzheimer's disease

CTRL – control

DAG – diacylglycerol

DIV – day of in vitro cultivation

ER – endoplasmic reticulum

HPF – Hyperforin

IBS – InterBioScreen

LTP – long-term potentiation

MS – mushroom spines

NSN21778 – N-{4-[2-(6-amino-quinazolin-4-ylamino)-ethyl]-phenyl}-acetamide

nSOCE – neuronal store-operated calcium entry

OAG – 1-Oleoyl-2-acetyl-sn-glycerol

Pa – probability to be active

PASS – Prediction of Activity Spectra for Substances

(<http://www.way2drug.com/passonline>)

Pi – probability to be inactive

PPZ – piperazine

TRPC6 – transient receptor potential canonical 6

## Abstract

Alzheimer's disease is the neurodegenerative disorder that is a major cause of dementia in the elderly. There is no cure against AD. We have recently discovered novel TRPC6-mediated intracellular signaling pathway that regulates stability of dendritic spines and plays a role in memory formation. We have previously shown that TRPC6 agonists exert beneficial effects in models of AD and may serve as lead compounds for development of AD therapeutic agents. In the current study, we used Integrity database to search for additional TRPC6 agonists. We have selected four compounds to study them as potential neuroprotective agents. We applied bioinformatics analyses to test basic pharmacological properties of selected compounds. We performed in vitro screening of these compounds to validate their ability to protect mushroom spines from amyloid toxicity and determined that two of these compounds exert neuroprotective effects in the nanomolar concentration range. We have chosen one of these compounds (piperazine, PPZ) for further testing. In agreement with previously published data, we have shown that PPZ potentiates TRPC6 channels. We demonstrated that neuroprotective mechanism of investigated PPZ is based on activation of neuronal store-operated calcium entry (nSOCE) in spines. We have shown that PPZ restores long-term potentiation (LTP) induction in 6 months old 5xFAD mouse hippocampal slices. Obtained results suggest that PPZ and its derivatives are potential lead molecules for development of AD therapeutic agents.

## Introduction

Alzheimer's disease (AD) is a neurodegenerative disease that occurs in aged people. The progressive death of nerve cells and, at the same time, the gradually increasing atrophy of the brain regions (hippocampus and cortex) are characteristic symptoms for AD. Human population is getting old due to increase in lifespan. This ultimately leads to increased frequency of neurodegenerative diseases. AD affects both the human mentality (loss of memory and eventually dementia) and ability of humans to serve themselves. Thus, the social significance of this problem is obvious. Besides, the treatment of neurodegenerative diseases is very expensive and constitutes a financial problem for society.

Dominant idea in AD field is the “amyloid hypothesis” that proposes that accumulation of beta-amyloid protein (A $\beta$ ) oligomers in patient's brain causes synaptic loss and eventually death of nerve cells (Hardy and Higgins, 1992) (Cline et al., 2018; Hardy and Selkoe, 2002; Selkoe and Hardy, 2016) Based on this hypothesis a number of therapeutic approaches have been tested, such as inhibitors of A $\beta$  production ( $\gamma$ -secretase and  $\beta$ -secretase inhibitors) and antibodies against A $\beta$  that can clear amyloid from the brain. However, so far all these clinical trials failed (Karran and Hardy, 2014). No new medications were approved by FDA for AD since 2003, and currently approved AD medications such as Memantine, Donepezil, Galantamine, and Rivastigmine only lead to a temporary symptomatic improvement in the status of patients.

It is known that in the early stages of the disease, before the appearance of toxic amyloid plaques, there is a loss of synapses in the neurons of patients with AD (Selkoe, 2002). Therefore, the existence of drugs that can slow or prevent the loss of synapses can significantly reduce the rate of development of neurodegenerative diseases, in particular Alzheimer's disease. In addition to accumulation of amyloid, AD neurons also display abnormal calcium (Ca<sup>2+</sup>) signaling (Bezprozvanny and Mattson, 2008). Excess cytosolic Ca<sup>2+</sup> is toxic to cells and to

protect themselves, neurons trigger protective mechanisms aimed at restoring intracellular  $\text{Ca}^{2+}$  to normal levels. In our previous studies, we found that endoplasmic reticulum (ER)  $\text{Ca}^{2+}$  levels are increased in AD neurons, resulting in compensatory downregulation of neuronal store-operated calcium entry (nSOCE) (Sun et al., 2014; Zhang et al., 2015). Based on these findings we concluded that therapeutic agents that can facilitate nSOCE can prevent synaptic loss and slow down the progression of the disease at early stages. Using genetic approaches, we validated this idea in presenilin knock-in model AD (PS1-M146V-KI) (Sun et al., 2014) and in APP knock-in (APP-KI) and amyloid toxicity models of AD (Popugaeva et al., 2015; Zhang et al., 2015). In more recent study, we identified the molecular identity of the channels carrying out the nSOCE (Zhang et al., 2016). We established that TRPC6 channels play a critical role in mediating nSOCE in hippocampal spines and demonstrated that hyperforin, a known activator of TRPC6, exerts synaptoprotective effects in PS-KI and APP-KI models (Zhang et al., 2016). These results are consistent with previous reports regarding beneficial effects of hyperforin and its derivatives in AD mouse models (Cerpa et al., 2010; Dinamarca et al., 2006; Griffith et al., 2010; Inestrosa et al., 2011). Based on these results we concluded that TRPC6 channel activators may have a beneficial effects in AD. This conclusion is consistent with increased excitatory synaptic density in TRPC6 transgenic mice (Zhou et al., 2008) and with reduced TRPC6 expression levels in blood cells from AD patients (Lu et al., 2018). Notably, TRPC channels emerge as potential targets for treatment of variety of psychiatric and neurological disorders (Bon and Beech, 2013; Zeng et al., 2016).

In previous studies, we identified a molecule that acts as positive modulator of TRPC6 activity and activator of nSOCE. This compound, called NSN21778, was able to restore mushroom synaptic spine and rescue long-term potentiation (LTP) defect in PS1-KI and APP-KI models of AD (Zhang et al., 2016). However, we also found that the NSN compound has poor pharmacokinetics and poorly penetrates the blood-brain barrier (Zhang et al., 2016). Thus,

in the present study we focused on search for additional TRPC6 activators and positive modulators. To achieve this goal, we applied bioinformatics approaches to identify potential TRPC6 activators. Identified compounds were tested in spine rescue assay with neuronal cultures challenged with A $\beta$  oligomers. Based on *in vitro* screen we selected a lead compound and demonstrated that this compound rescues LTP defects in 5xFAD mouse model of AD. We propose that this compound and its analogs may be useful for development of AD therapeutic agents. The mechanism of action of such agents is focused on synaptic stabilization, and it is complementary with anti-amyloid approaches.

## Material and methods

### Chemical compounds

51164 (N-(2-chlorophenyl)-2-(4-phenylpiperazin-1-yl)acetamide), 50741 (N-(4-fluorophenyl)-2-(4-(o-tolyl)piperazin-1-yl)acetamide), 64402 (1,1'-(4,6-dihydroxy-1,3-phenylene)bis(propan-1-one)) were obtained from public chemical library InterBioScreen (Chernogolovka, Russia). Hyp9 (1,1'-(2,4,6-Trihydroxy-1,3-phenylene)bis-1-hexanone) was obtained from Sigma Aldrich (H9791).

### Molecular biology reagents

Lenti-TRPC6, lenti-TRPC6-shRNAi, lenti-Ctrl-shRNAi plasmids were previously described (Zhang et al., 2016). pCSCMV:tdTomato plasmid was a gift from Gerhart Ryffel (Addgene plasmid # 30530) (Waldner et al., 2009).

### Bioinformatical analyses

In silico predictions were carried out using the retrained version of PASS for potential agonists of TRPC6 channels. PASS is a software product for the prediction of biological activity spectra for chemical compounds on the basis of their structural formula. In the current study online version of the PASS program has been used (<http://www.way2drug.com/passonline>). Structural formulas were presented as MOL files. Prediction of this spectrum by PASS is based on Structure-Activity Relationships (SAR) analysis of the training set containing about one million compounds showing more than 7000 biological activities. The PASS approach has been previously described in detail (Filimonov et al., 2014). In the PASS training set as “active” compounds are considered compounds having the quantitative characteristics of activity better than  $10^{-4}$  M. All the other compounds which are less active or their activity is unknown are considered as “inactive.” The PASS user obtains output information as a list of predicted types



of activity with the estimated probability for each type of activity: “to be active”  $P_a$  and “to be inactive”  $P_i$ . The probabilities  $P_a$  and  $P_i$  also indicate the estimated probabilities of first-kind and second-kind errors, respectively (Filimonov et al., 2014).  $P_a$  and  $P_i$  values vary from 0.000 to 1.000 and, in general,  $P_a \neq 1 - P_i$ , since these probabilities are calculated independently. For  $P_a > 90\%$ , we risk missing about 90% of actually active compounds but the probability of false-positive predictions is insignificant. For  $P_a > 80\%$ , we miss only 80% of the active compounds but the probability of false-positive predictions will be higher, and so forth. Finally, for  $P_a = P_i$ , the probabilities of false-positive and false-negative errors will be equal (Filimonov et al., 2014). It should be noted that the probability  $P_a$  primarily reflects the similarity of the structure of a given molecule to the structures of molecules of the most typical active compounds in the corresponding subset of the training set. Thus, there is no direct correlation of the values of  $P_a$  with quantitative activity characteristics. A really active molecule possessing molecular structure atypical for the training set may have a low  $P_a$  value in the prediction, perhaps even  $P_a < P_i$ . Another important aspect of interpreting the prediction results is related to novelty of the analyzed compound. If we limit ourselves only to activity types predicted with the highest values of  $P_a$ , the compounds selected by the prediction may prove to be analogs of known pharmacological agents. For example, when  $P_a > 0.7$ , the chances of finding experimental activity are rather high but the compounds found may be close structural analogs of known drugs. If we select in the range  $0.5 < P_a < 0.7$ , the chances for detecting experimental activity will be lower but the compounds will be less similar to known pharmaceutical agents. For  $P_i < P_a < 0.5$ , the chances of detecting experimental activity will be even lower, but if the prediction is confirmed, the compound found may prove a parent compound for a new chemical class for the biological activity examined (Filimonov et al., 2014).

## **Mice**

Albino outbred mice (Rappolovo farm, Leningradsky District, Russia) or inbred WT mice (C57BL/6J background) obtained from the Jackson Laboratory, USA (Stock Number: 000664) were used as a source of brain tissue for experiments with hippocampal cultures. For LTP induction experiments mice of 5xFAD mouse line (Oakley et al., 2006) (Stock Number: 006554 from the Jackson Laboratory, USA) were used at the age of 2 and 6 months. Control mice were age-matched WT littermates. All mouse experiments have been performed according to the procedures approved by the local animal control authorities.

## **Mice genotyping**

The presence of the transgene in 5xFAD mice was checked using a genotyping technique. The necessary DNA material was obtained from the tip of the animal's tail. The tip was then placed in 125  $\mu$ l of a SNET buffer (20 mM Tris-HCl, 5 mM EDTA, 400 mM NaCl, 1% SDS (pH 8)) with an addition of 10  $\mu$ l of K proteinase dissolved in water at a concentration of 10 mg/ml and incubated at a temperature of 55 °C for 2 to 16 h. Next 160  $\mu$ l of phenol/chloroform/isoamyl alcohol was added to the reaction mixture in a ratio of 25:24:1. The content of the test tube was mixed thoroughly and centrifuged at 14,000 rpm for 10 min at room temperature. The upper fraction containing the DNA was transferred to a clean tube and stored at a temperature of +4 °C. The presence of the transgene was checked by polymerase chain reaction (PCR) using primers specific to the insertion causing the expression of the transgenic (human) genes PSEN1 and APP in individual brain neurons. We used the following primers: The primer pair for determining the PSEN1 transgene: 5' AAT AGA GAA CGG CAG GAG CA 3' and 5' GCC AT G AGG GCACT AAT CAT 3'. The primer pair for determining the APP transgene: 5' AGG ACT GAC CACT CG ACC AG 3' and 5' CGG GGG T CT AGT T CT GCA T 3'. The

control primer pair: 5' CT A GGC CAC AGA AT T GAA AGA T CT 3' and 5' GT A GGT GGA AAT T CT AGC AT C AT C C 3'.

### **A $\beta$ 42 preparation**

A $\beta$ 42 (#20276) peptides were purchased from AnaSpec (Fremont, USA). A lyophilized aliquot (1 mg) of A $\beta$ 42 and A $\beta$ 40 peptides was dissolved in 80  $\mu$ l of 1% NH<sub>4</sub>OH and then in 920  $\mu$ l of sterile phosphate-buffered saline (PBS) to get stock solution with concentration 1 mg/ml (stored as 100  $\mu$ l aliquots at – 20°C). Working A $\beta$  solutions were made immediately before treatment of the cells by diluting stock concentration to 0.1  $\mu$ M final A $\beta$  peptide concentrations in Neurobasal-A medium (Gibco, Life Technologies, USA). Working

solutions were incubated at +4°C 24 hours to obtain the oligomeric conditions as described by Zheng et al. (Zheng M, 2012). On the day of the usage working solutions were centrifuged at 14000 g, + 4°C, 10 min to purify oligomeric A $\beta$  fraction from fibrils. The composition of supernatant fraction was previously confirmed by denaturing (0,1 %SDS) 15% gel electrophoresis followed by Western blot with anti-A $\beta$  6E10 monoclonal antibodies (Covance, SIG-39320) (Popugaeva et al., 2015). The supernatant fractions containing A $\beta$  oligomers were used to treat hippocampal cultures.

### **Primary hippocampal cultures**

The hippocampal cultures from albino outbred mice were established from postnatal day 0–2 pups and maintained in culture as we described previously (Popugaeva et al., 2015; Sun et al., 2014; Zhang et al., 2010). Both hippocampi from pups were dissected in sterile ice cold 1XHBSS buffer (pH 7,2). Hippocampi were dissociated in papain solution (Worthington 3176) at 37°C, 30 min. To remove big undissociated cell aggregates solution with hippocampal neurons were twice triturated in 1  $\mu$ g/ml DNaseI (Sigma, DN-25). To remove DNaseI neurons were centrifuged at 1500rpm, 4 min. Supernatants discarded and fresh warm (37 °C) growth

medium (Neurobasal-A (Gibco, 10888), 1xB27 (Gibco, 17504), 1% heat-inactivated FBS (Gibco, 16000), 0.5 mM L-Glutamine (Gibco, 25030)) was added. Neurons were plated in 24 well plate containing 12 mm round Menzel cover slip (d0-1) precoated with 1% poly-D-lysine (Sigma, p-7886). Neurons were seeded at  $\sim 5 \times 10^4$  cells per well (24 well format). Growth medium was changed on the next day after plating then weekly. In control experiments neuronal cultures were treated with equivalent amount (same volume as used to prepare A $\beta$  solutions) of Neurobasal A incubated at +4°C 24 hours (vehicle).

### **Calcium-phosphate transfection of primary hippocampal cultures**

Calcium-phosphate transfection of primary hippocampal cultures was done as previously described (Sun et al., 2014; Zhang et al., 2010). Changes to published protocol were in following steps: the volume of transfection reaction added to each well was 25 $\mu$ l. When GCamp5.3: TRPC6-si/CTRL-si co-transfection was performed the DNA ratio was 1:3.

### **Dendritic spine analysis in primary hippocampal neural cultures**

For assessment of synapse morphology, hippocampal cultures were transfected with TD-tomato plasmid at DIV7 using the calcium phosphate method and fixed (4% formaldehyde in PBS, pH 7.4) at DIV14. A Z-stack of optical section was captured using 100X objective (Olympus, UPlanSApo) with a confocal microscope (Thorlabs, USA). Each image maximal resolution was  $1024 \times 1024$  pixels with 0.1  $\mu$ m/pixel and averaged six times. Total Z volume was 6 – 8  $\mu$ m imaged with Z interval 0.2  $\mu$ m. At least 18 transfected neurons for each treatment from three independent experiments were used for quantitative analysis. Quantitative analysis for dendritic spines was performed by using freely available NeuronStudio software package (Rodriguez et al., 2008) as we previously described (Sun et al., 2014). To classify the shape of neuronal spines in culture, we adopted an algorithm from the published method (Rodriguez et al., 2008). In classification of spine shapes we used the following cutoff values: aspect ratio for thin spines

(AR<sub>thin</sub>(crit)) = 2.5, head to neck ratio (HNR(crit)) = 1.4, and head diameter (HD(crit)) = 0.45  $\mu\text{m}$ , the Z interval was 0.2  $\mu\text{m}$ . These values were defined and calculated exactly as described by a previous report (Rodriguez et al., 2008).

### **Fura-2 Ca<sup>2+</sup> imaging experiments**

Fura-2 Ca<sup>2+</sup> imaging experiments of HEK293T cells were performed as previously described (Zhang et al., 2016). Briefly, HEK293 cells were transfected with EGFP plasmid or a mixture of EGFP and TRPC6 plasmids (at 1:5 ratio), cultured for 40 – 48 h, and loaded with Fura2-AM. Fura-2 340/380 ratio images were collected using a DeltaRAM-X illuminator, Evolve camera, and IMAGEMASTER PRO software (all from Photon Technology International) from GFP-positive cells. To test the direct effect of HPF or 51164, the cells were loaded with Fura-2 and incubated in artificial CSF (aCSF) containing the following (in mM): 140 NaCl, 5 KCl, 1 MgCl<sub>2</sub>, 2 CaCl<sub>2</sub>, and 10 HEPES, pH 7.3. After basal recordings for 30 s, 10  $\mu\text{M}$  HPF or 30  $\mu\text{M}$  compound 51164 were applied and Ca<sup>2+</sup> responses measured by Fura-2. To test the effect of compound 51164 on OAG response, cells were moved to aCSF medium containing 0.1 mM Ca<sup>2+</sup> for 2 min and then returned to aCSF medium containing 2 mM Ca<sup>2+</sup> and 50  $\mu\text{M}$  OAG. These experiments were performed in the absence or presence of 30  $\mu\text{M}$  of compound 51164. The maximal amplitude (peak) of Ca<sup>2+</sup> influx was determined from the Fura-2 340 nm/380 nm ratio. All Ca<sup>2+</sup> imaging experiments were performed at room temperature.

### **GCamp5.3 Ca<sup>2+</sup> imaging experiments**

GCamp5.3 Ca<sup>2+</sup> imaging experiments were performed as we described previously (Zhang et al., 2015) with some changes in protocol. Cultured hippocampal neurons were transfected with GCamp5.3 expression plasmid using the calcium phosphate transfection method at DIV7. Calcium imaging experiments were performed in steady bath. GCamp5.3 fluorescent images were collected using Thorlabs upright confocal microscope equipped with a 60x/ 1.00 W lens

LUMPlanFL N (Olympus). The experiments were controlled by Thorimage LS 1.4 image acquisition software package (Thorlabs). To measure spine nSOCE, neurons were moved from aCSF to calcium-free medium containing following drugs 400  $\mu$ M EGTA; 1  $\mu$ M Thapsigargin, 10  $\mu$ M D-AP5, 50  $\mu$ M Nifedipine, 10  $\mu$ M CNQX, 1  $\mu$ M TTX for 30 min. Then neurons were subjected to addition of the 5  $\mu$ l 2 mM  $Ca^{2+}$ . In the case when the effect of agonist of TRPC6 channels was studied it has been added to the bath with other drugs. Analysis of the data was performed using ImageJ software. The region of interest used in the image analysis was chosen to correspond to spines. All  $Ca^{2+}$  imaging experiments were performed at room temperature.

### **Hippocampal slice preparation**

The mice were decapitated, and their brains were rapidly removed. The cerebellum and a small section of frontal cortex were removed. Flat surface for mounting the brain was created by making blocking cut on the dorsal surface parallel to the horizontal plane. The brain was then mounted onto the stage of a vibratome HM 650V (Microm International, Germany), and horizontal sections (400  $\mu$ m thick) were cut in ice-cold (0°C) artificial cerebrospinal fluid (ACSF). ACSF composed of (in mM) 126 NaCl, 2.5 KCl, 1.25  $NaH_2PO_4$ , 1  $MgSO_4$ , 2  $CaCl_2$ , 24  $NaHCO_3$ , and 10 glucose was bubbled with carbogen (95%  $O_2$ /5%  $CO_2$ ). The prepared slices were immersed in a chamber with aerated ACSF, which was placed into a temperature controlled water bath (35°C) for 1 h. After the incubation, the slices were transferred to the recording chamber, where they were kept for 15-20 min prior to the electrophysiological study. In this chamber, hippocampal slices were perfused with a constant flow of oxygenated ACSF at a rate of 5 mL/min at room temperature. One to five slices from each mouse were used in the experiment.

### **Electrophysiological recordings**

Field excitatory postsynaptic potentials (fEPSPs) were recorded from CA1 stratum radiatum using glass microelectrodes (0.2-1.0 M $\Omega$ ) filled with ACSF. Synaptic responses were evoked

by local extracellular stimulation of the Schaffer collaterals using a tungsten bipolar electrodes (Microprobes for Life Science, USA) placed in the stratum radiatum at the CA1–CA2 border. The stimulation was performed with rectangular paired pulses (duration, 0.1 ms; interstimulus interval, 50 ms) every 20 s. The dependence of field response amplitude on stimulation strength was determined by increasing the current intensity from 20 to 200  $\mu$ A via an A365 stimulus isolator (WPI, USA). The stimulus intensity used in the experiment was chosen so that the amplitude of fEPSPs would be 40-50% of the amplitude where the population spike appeared for the first time. The strength of stimulation was unvaried during the experiments, usually being 50-150  $\mu$ A. For each fEPSP, the amplitude and the slope of the rising phase at a level of 20-80% of the peak amplitude were measured. The LTP induction was started only if a stable amplitude of the baseline fEPSP had been recorded for 20 min. LTP was induced by theta-burst stimulation (TBS) protocol consisted of five bursts of five 100 Hz pulses, with a 200 ms interval between bursts, applied five times every 10 s. The fEPSPs were recorded after induction protocol during 40 min. Responses were amplified using an amplifier model 1800 (A-M Systems, USA) and were digitized and recorded on a personal computer using ADC/DAC NI USB-6211 (National Instruments, USA) and software (WinWCP v5.2.2, USA). Electrophysiological data were analyzed with the Clampfit 10.2 program (Axon Instruments, USA). The baseline fEPSPs and the potentiated fEPSPs (recorded 30-40 min after TBS) were averaged separately to measure LTP. Plasticity value was calculated as a ratio of the slope of the rising phase in the averaged potentiated and baseline fEPSPs.

### **Statistical analyses**

The results are presented as mean $\pm$ standard deviation (SD). The statistical significance was assessed by a one-way ANOVA following Dunnett's post hoc test, a two-way repeated measures ANOVA following Tukey's post hoc test or Kruskal-Wallis ANOVA where

appropriate. The p values are indicated in figure legends as appropriate. The data were processed with Statistica 8.0 (StatSoft, USA) and OriginPro 8.



## Results

### Bioinformatics search for TRPC6 activators

In our search we focused on finding the TRPC6 activators that differ in structure from NSN21778 compound. Using the Intergrity database (Clarivate Analytics), we have searched for known ligands of TRPC6 channels (agonists and antagonists). We have found six potential activators of TRPC6 (Table 1, Supplemental Integrity product report). The Integrity IDs of these compounds are HYP-1, HYP-5, HYP-9, 830288, 871099 and 880395. However, most of these molecules, except HYP-9 (Fig 1A), were not available for experimental testing. Therefore, we searched for chemical analogs of these molecules in public chemical libraries. As a result of this search we identified several analogs in the InterBioScreen chemical library (IBS, Chernogolovka, Russia) (Supplemental List 1). We selected four candidate compounds from this list based on the high percentage ( $\geq 88\%$ ) of coincidence with the structures of the desired compounds. These compounds are 64402 (analog of HYP-1), 50741 (analog of 880395) and 51164 (analog of 871099) (Fig 1B, 1C, 1D, Table 2)

By using PASS program, we evaluated the biological activity, toxicity, and mutagenicity of HYP-9 and 3 compounds from the IBS database (64402, 50741 and 51164). PASS program utilizes only structural data to predict activity of the compound. TRPC6 is a novel target for pharmacological studies, and it is unlikely to identify “TRPC6 agonist” biological activity by the PASS software. Instead we were searching for compounds that demonstrate some activity towards calcium channels. We were also interested in working with compound that do not possess adverse and toxic effects or at least demonstrate moderate toxicity. According to the PASS data (Table 2) all four compound demonstrate abilities to activate voltage-sensitive calcium channels with probability of activity  $P_a$  in the range from 0.49 to 0.624, with the maximum value for compound 51164 and the minimum value for 50741.

PASS program has shown another biological activity named “Calcium channel activator” (Table 2). Probability of activity Pa to activate calcium channels was in the range from 0.22 to 0.368, with the maximum value for compound 51164 and the minimum value for Hyp9 (Table 2). PASS online software allows to estimate probable adverse and toxic effects of selected compounds. 50741 and 51164 compounds are not predicted to demonstrate such toxic effects as carcinogenic, cardiodepressant or vascular/respiration toxicity showing Pa values near 0.2 (Table 2). However, 51164 is predicted to demonstrate such adverse effects as gastrointestinal hemorrhage and multiple organ failure with Pa values in the range from 0.56 to 0.78 (Table 2). 50741 is predicted to have moderate adverse effect with Pa 0.38 for gastrointestinal hemorrhage and Pa 0.39 for multiple organ failure (Table 2). In contrast Hyp9 and 64402 compounds are predicted to demonstrate moderate carcinogenic and cardiodepressant activities with Pa values in the range from 0.30 to 0.49 (Table 2). In addition both Hyp9 and 64402 compounds are predicted to demonstrate high adverse and toxic effects such as gastrointestinal hemorrhage and multiple organ failure with Pa values in the range from 0.60 to 0.88 (Table 2).

### **Validation of biological activities of selected compounds – potential agonists of TRPC6**

Previously we developed *in vitro* model of amyloid synaptotoxicity (Popugaeva et al., 2015). We have shown that this model is a useful tool for validating molecules that are able to protect synaptic spines from amyloid synaptotoxicity. Thus, we used this model as a screening assay to validate the neuroprotective effects of selected compounds. Previously we have shown that Hyperforin (HPF) at 30 nM concentration protects mushroom spines in APP-KI neurons (Zhang et al., 2016). It has been previously shown that HPF is direct activator of TRPC6 channels (Leuner et al., 2007). Thus, HPF has been used as positive control in our experiments.

We started the validation process from the known activator of TRPC6, compound HYP9 (Leuner et al., 2010). At 100 nM concentration HYP9 there was a trend in the ability of Hyp9 to protect mushroom spines from amyloid toxicity although it did not reach a level of statistical significance (%MS in A $\beta$ 42 group 10 $\pm$ 4% in comparison to %MS in A $\beta$ 42+HYP9 100nM group 14 $\pm$ 3%,  $p > 0.05$  by one way ANOVA with Dunn-Sidak post hoc,  $n$  (neurons)  $\geq 16$  from two independent cultures (Fig 2A, 2B). At 1  $\mu$ M concentration HYP9 did not protect mushroom spines from amyloid toxicity in our experiments (% MS in A $\beta$ 42 group 10 $\pm$ 4% in comparison to %MS in A $\beta$ 42+HYP9 1  $\mu$ M group 10 $\pm$ 6%,  $p > 0.05$  by one way ANOVA with Dunn-Sidak post hoc,  $n \geq 16$  neurons from two independent cultures, Fig 2A, 2B). As expected from our previous studies (Zhang et al., 2016) HPF protected mushroom spines from amyloid toxicity at 300 nM concentration (%MS in A $\beta$ 42 group 10 $\pm$ 4% in comparison to %MS in A $\beta$ 42+HPF 300nM group 20 $\pm$ 3%,  $p = 0.028$  by by one way ANOVA with Dunn-Sidak post hoc,  $n \geq 16$  neurons from two independent cultures) (Fig 2A, 2B).

Next we tested 64402 compound that has the highest percentage of similarity (91%) to the structure of HYP-1 (known activator of TRPC6 (Leuner et al., 2010)) (Table 2). We determined that compound 64402 did not show neuroprotective effect at the concentration of 1  $\mu$ M (%MS in A $\beta$ 42 group 10 $\pm$ 4% in comparison to %MS in A $\beta$ 42+64402 1 $\mu$ M 9 $\pm$ 5%,  $p > 0.05$  by one way ANOVA with Dunn-Sidak post hoc,  $n$  (neurons)  $\geq 16$  from two independent cultures, Fig 2A, 2B).

Next we tested 50741 compound that shows high percentage of similarity (90.24%) with a known TRPC6 activator compound 880395 from the Integrity database (Table 2). We have observed that compound 50741 demonstrates neuroprotective effects at concentrations 10 nM and 30 nM, recovering percent of mushroom spines in A $\beta$ 42-treated group from 21 $\pm$ 10% to 37 $\pm$ 2% and 47 $\pm$ 2%, respectively ( $p < 0.0001$  by two way ANOVA with Dunn-Sidak post hoc test,  $n$  (neurons)  $\geq 46$  from three independent cultures, Fig 3A, 4B). At 1 nM concentration

compound 50741 did not protect hippocampal neurons from A $\beta$ 42 toxicity (%MS A $\beta$ 42+50741 1 nM group 22 $\pm$ 2%, n (neurons)  $\geq$  46, Fig 3A, 4B).

Next we tested 51164 compound that shows 88% similarity to compound 871099 from Integrity database (Table 2). We discovered that at 10 nM concentration compound 51164 fully rescued mushroom spines in A $\beta$ 42-treated neurons (%MS is 49 $\pm$ 1%, n (neurons)  $\geq$  46), Fig 4A, 4B). This compound was also active in 30 nM and 100 nM concentrations (Fig 4A, 4B). It lost its activity at 1 nM concentration (%MS in A $\beta$ 42+51164 1 nM group is 23 $\pm$ 2%, %, n (neurons)  $\geq$  46, Fig 4A, 4B). Based on obtained results we have chosen 51164 as a lead compound for further investigation as synaptoprotective activity of this compound was most robust in spine protection assay (Fig 4) and this compound was predicted to have a favorable toxicological profile (Table 2).

#### **Verification of TRPC6 channels as the target for compound 51164**

Compound 51164 is an analog of known from the literature activator of TRPC6 (derivative of piperazine - 871099). Next, we aimed to determine if compound 51164 is indeed able to activate calcium influx via TRPC6 channels. In these experiments we used previously established HEK cell lines that were transiently transfected either with GFP or TRPC6 expressing plasmids (Zhang et al., 2016). To evaluate effects of compound 51164 we performed a series of Fura-2 Ca<sup>2+</sup> imaging experiments. Hyperforin (HPF) was used as a positive control in these experiments. In standard recording conditions (2 mM extracellular Ca<sup>2+</sup> ) addition of 10  $\mu$ M HPF induced rapid and strong response in HEK-TRPC6 cell line (peak amplitude for HPF treated HEK-TRPC6 cells is 1.0  $\pm$ 0.2 a.u (n  $\geq$  40) (Fig 5A, 5B). In contrast, even 30  $\mu$ M of compound 51164 failed to elicit Ca<sup>2+</sup> response in HEK-TRPC6 cell line in these conditions (Fig 5A, 5B). Thus, compound 51164 does not appear to act as direct agonist of TRPC6 channels.

In our previous studies we demonstrated that NSN21778 compound potentiates activity of TRPC6 channels in conditions of store depletion and in OAG-dependent manner (Zhang et al., 2016). OAG is synthetic cell permeant analogue of DAG, a known activator of TRPC6 channels (Estacion et al., 2004). Thus, we have decided to investigate whether compound 51164 acts in a similar way. In these experiments HEK293 cells transfected with EGFP or EGFP+TRPC6 cells were incubated in conditions of partially depleted stores (0.1 mM extracellular  $\text{Ca}^{2+}$ ) for 2 minutes, and then the extracellular media was changed to solution containing 2 mM  $\text{Ca}^{2+}$  in the presence of 50  $\mu\text{M}$  OAG. Application of 50  $\mu\text{M}$  OAG by itself did not induce  $\text{Ca}^{2+}$  influx in EGFP transfected HEK cells (data not shown). EGFP-transfected HEK cells had small response to application of 50  $\mu\text{M}$  OAG in conditions of partial store depletion and this response was not affected by application of 30  $\mu\text{M}$  51164 (Fig 5C, 5D). In contrast, TRPC6-transfected HEK cells responded to response to application of 50  $\mu\text{M}$  OAG in conditions of partial store depletion (Fig 5C), with an average amplitude of the response equal to  $0.25 \pm 0.025$  a.u (n = 239) (Fig 5D). Application of 51164 compound at 30  $\mu\text{M}$  concentration facilitated  $\text{Ca}^{2+}$  response in TRPC6-transfected HEK cells in these conditions (Fig 5C), with an average response equal to  $0.45 \pm 0.05$  a.u (n = 214) (Fig 5D), significantly ( $p < 0.0001$  by two way ANOVA with Tukey post hoc) higher than in the absence of 51164 compound. Based on obtained results, we concluded that 51164 compound acts as a positive modulator of TRPC6 channels, a mechanism of action similar to NSN21778 compound.

### **51164 restores nSOCE in hippocampal neurons treated with A $\beta$ 42**

To investigate whether 51164 activates endogenous synaptic nSOCE we performed  $\text{Ca}^{2+}$  imaging experiments with hippocampal neuronal cultures transfected with GCamp5.3. At the day of imaging cover glasses with neurons were incubated in  $\text{Ca}^{2+}$ -free media in the presence

of  $\text{Ca}^{2+}$  channels inhibitors for 30 min. Following elevation of extracellular  $\text{Ca}^{2+}$  to 10 mM,  $\text{Ca}^{2+}$  influx was reported by GCamp5.3 (Fig 6A). An average size of the response observed in synaptic spines was  $6 \pm 2$  a.u. ( $n \geq 60$  spines from three independent cultures) (Fig 6J). These responses were significantly facilitated in the presence of 300 nM of Hyperforin (HPF), which was used as a positive control (Fig 6B). On average, the size of response in the presence of HPF was increased to  $10 \pm 1$  a.u. ( $n \geq 60$  spines from three independent cultures) (Fig 6J), significantly ( $p < 0.0001$  by Kruskal-Wallis ANOVA) higher than in control conditions. These data support an important role of TRPC6 channels in mediating spine nSOCE and in agreement with our previous observations (Zhang et al., 2016). In contrast,  $\text{Ca}^{2+}$  responses were not affected by the presence of 300 nM of compound 51164 (Fig 6C, 6J). Preincubation of hippocampal cultures with A $\beta$ 42 oligomers (100nM A $\beta$ 42 oligomers were present in culture for three days) downregulated nSOCE in hippocampal neurons (Fig 6D). An average amplitude of nSOCE in these conditions was  $4 \pm 1$  a.u. ( $n \geq 60$  spines from three independent cultures) (Fig 6J), significantly ( $p < 0.01$  by Kruskal-Wallis ANOVA) lower than in control conditions. Incubation with 300 nM HPF was able to restore the amplitude of nSOCE in A $\beta$ 42-treated cultures (Fig 6E), with an average amplitude of the response equal to  $10 \pm 4$  a.u. ( $n \geq 60$  spines from three independent cultures) (Fig 6J), significantly ( $p < 0.01$  by Kruskal-Wallis ANOVA) higher than in A $\beta$ 42-treated cultures alone. Incubation with compound 51164 was also able to restore nSOCE amplitude in hippocampal neurons treated with A $\beta$ 42 (Fig 6F). An average amplitude of nSOCE in the presence of compound 51164 was equal to  $6 \pm 1$  a.u. ( $n \geq 60$  spines from three independent cultures) (Fig 6J), that is the same as in control conditions and significantly ( $p < 0.05$  by Kruskal-Wallis ANOVA) higher than in A $\beta$ 42-treated cultures alone. To further confirm that TRPC6 is modulation of nSOCE by 51164 compound we transfected neuronal cultures with the plasmid expressing shTRPC6 RNAi. We have observed that the absence of TRPC6 caused downregulation of nSOCE amplitude in HPF and 51164 pretreated neurons to

4±1 and 3±1, respectively (with  $p < 0.0001$  by Kruskal-Wallis ANOVA) (Fig 6G, 6H, 6I). From these experiments, we concluded that compound 51164 is able to restore synaptic nSOCE in hippocampal neurons that is suppressed by incubation with A $\beta$ 42 oligomers.

### **51164 restores long-term potentiation (LTP) deficit in 6 months old 5xFAD mice**

Next, we evaluated the effects of compound 51164 in LTP experiments with hippocampal slices from 5xFAD mouse model. LTP was induced in hippocampal Schaffer collateral-CA1 synapses by TBS protocol. In agreement with published data, LTP induction was significantly affected in hippocampal slices from 5xFAD mice in an age-dependent manner (Kimura and Ohno, 2009; Oakley et al., 2006). No difference was found between 5xFAD and wild-type mice at 2 months of age (Fig. 7A, 7C), while 6-month-old 5xFAD mice showed significant impairment of LTP (Fig 7B). On average, 30 min after TBS stimulation relative fEPSP slope for WT slices was  $1.62 \pm 0.8$  a.u. ( $n = 8$  slices), and for 5xFAD it was  $1.25 \pm 0.2$  a.u. ( $n = 12$ ), significantly lower (Fig 7D,  $p = 0.04$ ). Incubation with 100 nM 51164 compound had no effect on LTP recorded in 2 months old wild-type or 5xFAD hippocampal slices (Fig 7A, 7B). Pretreatment of hippocampal slices from 6 months old animals with a 100 nM 51164 compound for 30 min had no significant effect on LTP in WT slices (Fig 7B, 7D,  $p = 0.99$ ). However, 30 min pretreatment with 100 nM 51164 compound completely rescued the LTP deficit in slices from 5xFAD mice (Fig 7B; no difference between WT and 5xFAD treated with 51164,  $p = 0.79$ ). On average, 30 min after TBS stimulation relative fEPSP slope for 5xFAD slices treated with 51164 compound was  $1.8 \pm 0.4$  a.u. ( $n = 9$ ), significantly higher ( $p = 0.02$ ) than in 5xFAD slices alone (Fig 7D). From these results, we concluded that exposure to 51164 compound was sufficient to rescue LTP defects in 6 months old 5xFAD mice.

## Discussion

We have previously demonstrated that downregulation of synaptic nSOCE mechanism may contribute to synaptic loss in AD (Popugaeva et al., 2015; Sun et al., 2014; Zhang et al., 2015). Moreover, we identified NSN21778 compound that is able to upregulate TRPC6-mediated nSOCE in the hippocampal neurons and demonstrated that this compound is able to prevent synaptic loss and rescue LTP defects in hippocampal neurons from AD mouse models (Zhang et al., 2016). However, there are some limitations in using NSN21778 compound as potential therapeutic agent. NSN21778 compound does not have optimal pharmacokinetic properties and has poor penetrance across blood brain barrier. Another known TRPC6 activator is hyperforin. Hyperforin is a natural product that has been demonstrated to beneficial effects in AD mouse models (Cerpa et al., 2010; Dinamarca et al., 2006; Griffith et al., 2010; Inestrosa et al., 2011). However, hyperforin is very difficult to synthesize and long-term incubation with hyperforin results in apoptosis of hippocampal neurons (Zhang et al., 2016). In the current study we focused on identification of TRPC6 activators that have a different chemical structure than NSN21778 or hyperforin. We reasoned that such molecules may provide novel leads for development of AD therapeutic agents.

We performed a bioinformatics search for potential TRPC6 agonists and modulators and identified 6 candidate molecules in Integrity database (Table 1). However, most of these molecules were not available for experimental testing. Therefore, we searched for chemical analogs of these molecules and identified several compounds in the InterBioScreen chemical library. Based on the highest percentage of coincidence with the structure of the desired compound we selected four candidate compounds from this list for testing (Fig 1A-1D). We performed further bioinformatics analysis of these compounds using PASS program



(Filimonov et al., 2014), and established that 50741 and 51164 compounds are not predicted to demonstrate such toxic effects as carcinogenic, cardiodepressant or vascular/respiration toxicity (Table 2). We exposed neuronal cultures to A $\beta$ 42 oligomers and evaluated ability of these 4 compounds to rescue A $\beta$ 42-induced loss of mushroom spines. In our experiments hyperforin (HPF) was used as a positive control, as it is a well established TRPC6 activator that can rescue mushroom spine loss in AD models (Zhang et al., 2016). Based on obtained results (Fig 2-4) we selected compound 51164 ((N-(2-chlorophenyl)-2-(4-phenylpiperazin-1-yl)acetamide)) as our lead molecule. This compound was able to rescue A $\beta$ 42-induced loss of mushroom spines in 10 nM concentration (Fig 4) and it also has a favorable toxicity profile as predicted by PASS (Table 2).

Compound 51164 is a derivative of piperazine (PPZ) (Fig 1D). It has been previously established that derivatives of PPZs activate TRPC6 channels (Bon and Beech, 2013), with the proposed mechanism of action related to activation of BDNF pathway (Sawamura et al., 2016). We evaluated ability of compound 51164 to activate TRPC6 channels in experiments with transiently transfected HEK cells. We discovered that this compound does not directly activates TRPC6 channels in standard recording conditions but acts as a positive modulator of OAG-activated TRPC6 channels (Fig 5). That is, mechanism of action of this compound is different from hyperforin and similar to NSN21778 (Zhang et al., 2016). The effective concentration of compound 51164 in these experiments (30  $\mu$ M) was similar to the concentration of PPZ2 compound needed to activate TRPC6 channels in similar experiments (Sawamura et al., 2016). Previous reports also suggested that PPZ1 and PPZ2 activate TRPC6 channels in DAG-dependent manner but require activation of BDNF signaling pathway for these effects (Sawamura et al., 2016). We further demonstrated that compound 51164 is able to restore synaptic nSOCE in hippocampal neurons exposed to A $\beta$ 42 (Fig 6).

These effects are similar to results that we obtained previously with NSN21778 (Zhang et al., 2016). It has been previously shown that PPZ derivatives are able to activate  $\text{Ca}^{2+}$  influx not only via TRPC6 channels, but via TRPC3 and TRPC7 channels as well (Sawamura et al., 2016). This observation is relevant for drug development since TRPC3 and TRPC7 channels are expressed in various brain regions such as cerebellum, olfactory bulb and brain stem are predominant isoform of TRPC channels (Zhang et al., 2016). We have not evaluated specificity of compound 51164 for TRPC6 isoform when compared to other TRPC isoforms.

To further evaluate the neuroprotective effects of 51164 compound, we performed a series of LTP experiments with hippocampal slices from 5x FAD mice. 5xFAD mice is an aggressive AD mouse model that displays amyloid accumulation and cognitive dysfunction as early as four months of age (Kimura and Ohno, 2009; Oakley et al., 2006). In agreement with published reports, we observed LTP defects in hippocampal slices from 6 months old 5x FAD mice (Fig 7). Preincubation of slices with 100 nM 51164 compound rescued these LTP defects (Fig 7), suggesting that this compound may have utility for treating synaptic plasticity disruptions in AD.

In conclusion, in the current study we identified and characterized a compound 51164 ((N-(2-chlorophenyl)-2-(4-phenylpiperazin-1-yl)acetamide)) as a potential lead molecule for AD therapeutic development. This compound is a derivative of piperazine, a class of molecules widely used to treat psychiatric disorders (Kersten and McLaughlin, 2015). Our data suggest that compound 51164 acts as a positive modulator of TRPC6 channels, leading to stabilization of hippocampal synaptic spines in conditions of amyloid toxicity and rescue of LTP defects in hippocampal slices from AD mouse model. Compound 51164 exerted neuroprotective effects in concentrations 10 – 100 nM and it is predicted to have a favorable toxicity profile. Thus, this

compound or its derivatives constitute a potential lead molecule for AD therapeutic development.

## Acknowledgments

We thank Dr. P. Plotnikova for administrative support. Dr. Ilya Bezprozvanny is a holder of the Carl J. and Hortense M. Thomsen Chair in Alzheimer's Disease Research.

### Authorship Contributions

*Participated in research design:* E. Popugaeva, V. Poroikov, I. Bezprozvanny, A. Zaitsev

*Conducted experiments:* D. Chernyuk, E. Popugaeva, H. Zhang, K. Pats, T. Postnikova

*Contributed analytic tools:* V. Poroikov, E. Fedorova

*Performed data analysis:* D. Chernyuk, E. Popugaeva, H. Zhang, T. Postnikova, V. Poroikov

*Wrote or contributed to the writing of the manuscript:* E. Popugaeva, I. Bezprozvanny, V. Poroikov, E. Fedorova, A. Zaitsev

## References

- Bezprozvanny I and Mattson MP (2008) Neuronal calcium mishandling and the pathogenesis of Alzheimer's disease. *Trends Neurosci* 31(9): 454-463.
- Bon RS and Beech DJ (2013) In pursuit of small molecule chemistry for calcium-permeable non-selective TRPC channels -- mirage or pot of gold? *Br J Pharmacol* 170(3): 459-474.
- Cerpa W, Hancke JL, Morazzoni P, Bombardelli E, Riva A, Marin PP and Inestrosa NC (2010) The hyperforin derivative IDN5706 occludes spatial memory impairments and neuropathological changes in a double transgenic Alzheimer's mouse model. *Current Alzheimer research* 7(2): 126-133.
- Cline EN, Bicca MA, Viola KL and Klein WL (2018) The Amyloid-beta Oligomer Hypothesis: Beginning of the Third Decade. *J Alzheimers Dis* 64(s1): S567-S610.
- Dinamarca MC, Cerpa W, Garrido J, Hancke JL and Inestrosa NC (2006) Hyperforin prevents beta-amyloid neurotoxicity and spatial memory impairments by disaggregation of Alzheimer's amyloid-beta-deposits. *Molecular psychiatry* 11(11): 1032-1048.
- Estacion M, Li S, Sinkins WG, Gosling M, Bahra P, Poll C, Westwick J and Schilling WP (2004) Activation of human TRPC6 channels by receptor stimulation. *The Journal of biological chemistry* 279(21): 22047-22056.
- Filimonov DA, Lagunin AA, Glorizova TA, Rudik AV, Druzhilovskii DS, Pogodin PV and Poroikov VV (2014) Prediction of the Biological Activity Spectra of Organic Compounds Using the Pass Online Web Resource. *Chem Heterocycl Com+* 50(3): 444-457.
- Griffith TN, Varela-Nallar L, Dinamarca MC and Inestrosa NC (2010) Neurobiological effects of Hyperforin and its potential in Alzheimer's disease therapy. *Current medicinal chemistry* 17(5): 391-406.
- Hardy J and Selkoe DJ (2002) The amyloid hypothesis of Alzheimer's disease: progress and problems on the road to therapeutics. *Science* 297(5580): 353-356.
- Hardy JA and Higgins GA (1992) Alzheimer's disease: the amyloid cascade hypothesis. *Science* 256(5054): 184-185.
- Inestrosa NC, Tapia-Rojas C, Griffith TN, Carvajal FJ, Benito MJ, Rivera-Dictter A, Alvarez AR, Serrano FG, Hancke JL, Burgos PV, Parodi J and Varela-Nallar L (2011) Tetrahydrohyperforin prevents cognitive deficit, A $\beta$  deposition, tau phosphorylation and synaptotoxicity in the APP<sup>swe</sup>/PSEN1 $\Delta$ E9 model of Alzheimer's disease: a possible effect on APP processing. *Translational psychiatry* 1: e20.
- Karran E and Hardy J (2014) A critique of the drug discovery and phase 3 clinical programs targeting the amyloid hypothesis for Alzheimer disease. *Annals of neurology* 76(2): 185-205.
- Kersten BP and McLaughlin ME (2015) Toxicology and management of novel psychoactive drugs. *J Pharm Pract* 28(1): 50-65.
- Kimura R and Ohno M (2009) Impairments in remote memory stabilization precede hippocampal synaptic and cognitive failures in 5XFAD Alzheimer mouse model. *Neurobiol Dis* 33(2): 229-235.
- Leuner K, Heiser JH, Derksen S, Mladenov MI, Fehske CJ, Schubert R, Gollasch M, Schneider G, Harteneck C, Chatterjee SS and Muller WE (2010) Simple 2,4-diacetylphloroglucinols as classic transient receptor potential-6 activators--identification of a novel pharmacophore. *Molecular pharmacology* 77(3): 368-377.

- Leuner K, Kazanski V, Muller M, Essin K, Henke B, Gollasch M, Harteneck C and Muller WE (2007) Hyperforin--a key constituent of St. John's wort specifically activates TRPC6 channels. *FASEB J* 21(14): 4101-4111.
- Lu R, Wang J, Tao R, Wang J, Zhu T, Guo W, Sun Y, Li H, Gao Y, Zhang W, Fowler CJ, Li Q, Chen S, Wu Z, Masters CL, Zhong C, Jing N, Wang Y and Wang Y (2018) Reduced TRPC6 mRNA levels in the blood cells of patients with Alzheimer's disease and mild cognitive impairment. *Molecular psychiatry* 23(3): 767-776.
- Oakley H, Cole SL, Logan S, Maus E, Shao P, Craft J, Guillozet-Bongaarts A, Ohno M, Disterhoft J, Van Eldik L, Berry R and Vassar R (2006) Intraneuronal beta-amyloid aggregates, neurodegeneration, and neuron loss in transgenic mice with five familial Alzheimer's disease mutations: potential factors in amyloid plaque formation. *J Neurosci* 26(40): 10129-10140.
- Popugaeva E, Pchitskaya E, Speshilova A, Alexandrov S, Zhang H, Vlasova O and Bezprozvanny I (2015) STIM2 protects hippocampal mushroom spines from amyloid synaptotoxicity. *Mol Neurodegener* 10(1): 37.
- Rodriguez A, Ehlenberger DB, Dickstein DL, Hof PR and Wearne SL (2008) Automated three-dimensional detection and shape classification of dendritic spines from fluorescence microscopy images. *PloS one* 3(4): e1997.
- Sawamura S, Hatano M, Takada Y, Hino K, Kawamura T, Tanikawa J, Nakagawa H, Hase H, Nakao A, Hirano M, Rotrattanadumrong R, Kiyonaka S, Mori MX, Nishida M, Hu Y, Inoue R, Nagata R and Mori Y (2016) Screening of Transient Receptor Potential Canonical Channel Activators Identifies Novel Neurotrophic Piperazine Compounds. *Molecular pharmacology* 89(3): 348-363.
- Selkoe DJ (2002) Alzheimer's disease is a synaptic failure. *Science* 298(5594): 789-791.
- Selkoe DJ and Hardy J (2016) The amyloid hypothesis of Alzheimer's disease at 25 years. *EMBO Mol Med* 8(6): 595-608.
- Sun S, Zhang H, Liu J, Popugaeva E, Xu NJ, Feske S, White CL, 3rd and Bezprozvanny I (2014) Reduced synaptic STIM2 expression and impaired store-operated calcium entry cause destabilization of mature spines in mutant presenilin mice. *Neuron* 82(1): 79-93.
- Waldner C, Roose M and Ryffel GU (2009) Red fluorescent *Xenopus laevis*: a new tool for grafting analysis. *BMC Dev Biol* 9: 37.
- Zeng C, Tian F and Xiao B (2016) TRPC Channels: Prominent Candidates of Underlying Mechanism in Neuropsychiatric Diseases. *Mol Neurobiol* 53(1): 631-647.
- Zhang H, Sun S, Herreman A, De Strooper B and Bezprozvanny I (2010) Role of presenilins in neuronal calcium homeostasis. *J Neurosci* 30(25): 8566-8580.
- Zhang H, Sun S, Wu L, Pchitskaya E, Zakharova O, Fon Tacer K and Bezprozvanny I (2016) Store-Operated Calcium Channel Complex in Postsynaptic Spines: A New Therapeutic Target for Alzheimer's Disease Treatment. *J Neurosci* 36(47): 11837-11850.
- Zhang H, Wu L, Pchitskaya E, Zakharova O, Saito T, Saido T and Bezprozvanny I (2015) Neuronal Store-Operated Calcium Entry and Mushroom Spine Loss in Amyloid Precursor Protein Knock-In Mouse Model of Alzheimer's Disease. *J Neurosci* 35(39): 13275-13286.
- Zheng M LJ, Ruan Z, Tian S, Ma Y, Zhu J, Li G. (2012) Intrahippocampal injection of A $\beta$ 1-42 inhibits neurogenesis and down-regulates IFN- $\gamma$  and NF- $\kappa$ B expression in hippocampus of adult mouse brain. *Amyloid* 20(1): 13-20.
- Zhou J, Du W, Zhou K, Tai Y, Yao H, Jia Y, Ding Y and Wang Y (2008) Critical role of TRPC6 channels in the formation of excitatory synapses. *Nat Neurosci* 11(7): 741-743.

### Footnotes

This work was supported by the National Institutes of Health grant [R01NS080152] (IB) (results depicted in Figure 5), Russian Science Foundation Grant [14-25-00024-II] (results depicted in Figures 2-4), by the state grant [17.991.2017/4.6] (IB) (results depicted in Figure 1 and Figure 6), supported in part by RFBR grant project No. [17-00-00408] (AZ) (results depicted in Figure 7), by the grant of President of Russian Federation [14.Y30.17.1043-MK] (EP) (results depicted in Table 1 and Table 2) and by the Russian State Academies of Sciences Fundamental Research Program for 2013-2020 (VP) (Integrity search and PASS Online support).



### Figure legends

**Fig 1. Chemical structures of potential TRPC6 modulators identified as a result of bioinformatics search.**

A, HYP-9 B, Compound 64402 C, Compound 50741 D, Compound 51164. Compounds 64402, 50741 and 51164 were found in InterBioScreen (IBS) library.

**Fig 2. Evaluation of protective effects of HYP9 and 64402 in conditions of amyloid**

**synaptotoxicity.** A, Representative confocal images of DIV14 hippocampal neurons transfected with TD-Tomato plasmid. Images for control cultures (CTRL) and cultures exposed to oligomeric A $\beta$ 42 (A $\beta$ ) are shown as indicated. Hyperforin (HPF) was added in concentration of 300 nM, HYP9 was tested in concentrations 100 nM and 1  $\mu$ M as indicated, 64402 was tested in 1  $\mu$ M concentration.

B, The average percentages of mushroom spines (% MS) in each experimental condition are present as mean $\pm$ SD ( $n\geq 16$  neurons for each group). Untreated hippocampal cultures (CTRL) are shown as filled bar. Open bars correspond to hippocampal cultures that were treated with oligomeric A $\beta$ 42. \*\*\*  $p < 0.0005$ , \*  $p < 0.05$  by one way ANOVA following Dunn-Sidak post hoc.

**Fig 3. Evaluation of protective effects of compound 50741 in conditions of amyloid synaptotoxicity.**

A, Representative confocal images of DIV14 hippocampal neurons transfected with TD-Tomato plasmid. Images for control cultures (CTRL) and cultures exposed to oligomeric A $\beta$ 42 (A $\beta$ ) are shown as indicated. Hyperforin (HPF) was added in concentration of 30 nM, compound 50741 was tested in concentrations 1 nM, 10 nM, 30 nM and 100 nM as indicated. Scale bar is 10  $\mu$ m.

B, The average percentages of mushroom spines (% MS) in each experimental condition are present as mean $\pm$ SEM (n=22-32 neurons for each group). Untreated hippocampal cultures (CTRL) are shown as filled bars. Open bars correspond to hippocampal cultures that were treated with oligomeric A $\beta$ 42 (A $\beta$ ). \*\*p<0.005, \*\*\*p <0.0005 by two way ANOVA with Dunn-Sidak post hoc test.

**Fig 4. Evaluation of protective effects of compound 51164 in conditions of amyloid synaptotoxicity.**

A, Representative confocal images of DIV14 hippocampal neurons transfected with TD-Tomato plasmid. Images for control cultures (CTRL) and cultures exposed to oligomeric A $\beta$ 42 (A $\beta$ ) are shown as indicated. Hyperforin (HPF) was added in concentration of 30 nM, compound 51164 was tested in concentrations 1 nM, 10 nM, 30 nM and 100 nM as indicated. Scale bar is 10  $\mu$ m

B, The average percentages of mushroom spines (% MS) in each experimental condition are present as mean $\pm$ SEM (n=22-32 neurons for each group). Untreated hippocampal cultures (CTRL) are shown as filled bars. Open bars correspond to hippocampal cultures that were treated with oligomeric A $\beta$ 42 (A $\beta$ ). \*p<0.05, \*\*\*p <0.0005 by two way ANOVA with Dunn-Sidak post hoc test.

**Fig 5. Compound 51164 acts as a positive modulator of TRPC6 channels.**

A, Time course of Fura-2 fluorescence  $\text{Ca}^{2+}$  signals (340/380 ratio) is shown for HEK293 cells transfected with EGFP + TRPC6 plasmids. Traces from individual cells are shown as thin grey lines, an average traces are shown as thick red lines. Cells were incubated in aCSF medium containing 2 mM  $\text{Ca}^{2+}$ . The time of addition of 10  $\mu\text{M}$  Hyperforin (HPF) or 30  $\mu\text{M}$  of compound 51164 is indicated by red bars above the Fura-2 traces.

B, Average amplitude of  $\text{Ca}^{2+}$  influx peak is shown as change in 340/380 Fura-2 ratio signals for the cells exposed to HPF or compound 51164. The results are presented as mean  $\pm$  SEM (n = 40 cells). \*\*\*p <0.0001 by two way ANOVA with Tukey post hoc test.

C, Time course of Fura-2 fluorescence  $\text{Ca}^{2+}$  signals (340/380 ratio) is shown for HEK293 cells transfected with EGFP (GFP) or EGFP + TRPC6 (TRPC6) plasmids as indicated. Traces from individual cells are shown as thin grey lines, an average traces are shown as thick red lines. Cells were moved to modified aCSF medium containing 0.1 mM  $\text{Ca}^{2+}$  for 2 min and then returned to the medium containing 2 mM  $\text{Ca}^{2+}$  with the addition of 50  $\mu\text{M}$  of OAG. The time of addition of 30  $\mu\text{M}$  51164 is indicated by red bars above the Fura-2 traces.

D, Average amplitude of  $\text{Ca}^{2+}$  influx peak is shown as change in 340/380 Fura-2 ratio signals for each group of cells tested in experiments shown on panel C. The results are presented as mean  $\pm$  SEM (n = 40 cells). \*\*\*p <0.0001 by two way ANOVA with Tukey post hoc test.

**Fig 6. Compound 51164 rescues A $\beta$ <sub>42</sub>-supressed nSOCE in hippocampal postsynaptic dendritic spines.**

A-I, The time course of GCaMP5.3 fluorescence signal changes in the spines of hippocampal neurons at DIV14. Neurons were pre-incubated in Ca<sup>2+</sup> free media and 10 mM Ca<sup>2+</sup> was added as indicated by a black bar above the traces. The experiments were performed in the presence of drug cocktail of Ca<sup>2+</sup> inhibitors as described in Methods. The presence of 300 nM Hyperforin (HPF) or 300 nM compound 51164 (51164) is indicated by above GCaMP5.3 traces. For each experimental group, individual spine (this grey lines) and average (thick red red lines) fluorescence traces are shown. Results with control (CTRL) neurons are shown on panels A, B, C. Results with neurons pre-incubated with A $\beta$ <sub>42</sub> oligomers (A $\beta$ ) are shown on panels D, E, F as indicated. Results depicted on panels A-F are obtained in the presence of control shRNA (CTRLsh). Results with neurons transfected with shTRPC6 (T6sh) plasmids are on panels G, H, I.

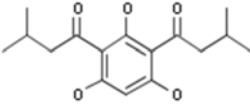
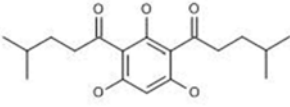
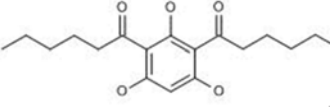
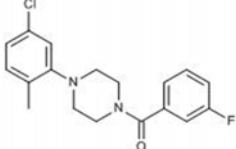
J, An average nSOCE spine peak amplitude is shown for each group of cells depicted on panels A-I. F/F<sub>0</sub> changes in GCaMP5.3 fluorescence are presented as mean  $\pm$  SD (n=20 spines),\* p<0.05, \*\*\*p<0.0005 by Kruskal-Wallis ANOVA.

**Fig 7. 51164 recovers LTP induction in slices from 6-month-old 5xFAD mice.**

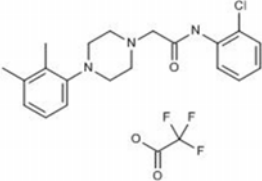
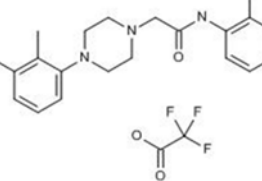
A, C, LTP is not altered in hippocampal slices from 2-month-old 5xFAD mice. Incubation of slices with the 100 nM 51164 does not influence LTP induction in slices from 2-month-old WT and 5xFAD mice (3-5 mice per group). Two-way ANOVA,  $F_{1,14} = 0.64$ ,  $p = 0.44$ . WT (n = 4 slices), WT(51164) (n = 5), 5xFAD (n = 3), 5xFAD (51164) (n = 6). B, D, LTP is impaired in hippocampal slices from 6-month-old 5xFAD mice. Incubation of 5xFAD slices from 6-month-old 5xFAD mice with the 100 nM 51164 recovers LTP induction. Two-way ANOVA following Tukey's post hoc test,  $F_{1,31} = 6.31$ ,  $p = 0.02$ . In 6 months old WT slices 51164 does not change LTP ( $p = 0.99$ ). WT (n = 8), WT (51164) (n = 6), 5xFAD (n = 12), 5xFAD (51164) (n = 9). \*  $p < 0.05$ ; \*\*  $p < 0.01$ .

## Tables

**Table 1.** The list of TRPC6 agonists from Integrity database (Thomson Reuters)

Integrity ID	IUPAC name	Structural formula	Molecular mechanism	Therapeutic group
HYP-1	2,4 - Bis(3 - methylbutyryl)phloroglucinol 2,4 - Bis(3 - methylbutyryl) - 1,3,5 - trihydroxybenzene		1) TRPC6 Agonists 2) Leukotriene CysLT1 (LTD4) Antagonists 3) Antagonists Free Fatty Acid Receptor 1 (FFAR1; PR40) 4) Agonists Signal Transduction Modulators 5) Prostanoid TP Antagonists 6) Leukotriene Antagonists	1) Antiallergy/ Antiasthmatic drugs 2) Antiviral 3) Agents for Type 2 Diabetes
HYP-5	1,1' - (2,4,6 - Trihydroxybenzene - 1,3 - diyl)bis(4 - methylpentan - 1 - one)		1) TRPC6 Agonists	1) Treatment of cognition disorders
HYP-9	1,1' - (2,4,6 - Trihydroxybenzene - 1,3 - diyl)dihexan - 1 - one		1) TRPC6 Agonists	1) Treatment of cognition disorders
830288	[4 - (5 - Chloro - 2 - methylphenyl)piperazin - 1 - yl](3 - fluorophenyl)methanone		1) TRPC6 Agonists	1) Psychiatric disorders (Not Specified)



				2) Treatment of neurodegenerative diseases
871099	N - (2 - Chlorophenyl) - 2 - [4 - (2,3 - dimethylphenyl)piperazin - 1 - yl]acetamide trifluoroacetate		1) TRPC6 Agonists 2) TRPC3 Agonists	1) Psychiatric disorders (Not Specified) 2) Treatment of neurodegenerative diseases
880395	2 - [4 - (2,3 - Dimethylphenyl)piperazin - 1 - yl] - N - (2 - fluorophenyl)acetamide trifluoroacetate		1) TRPC6 Agonists 2) TRPC3 Agonists	1) Psychiatric disorders (Not Specified) 2) Treatment of neurodegenerative diseases

**Table 2.** Biological activities of selected compounds predicted by PASS online web service

Mechanism of action

Compound number	<u>Hyp9</u>		<u>64402</u>		<u>50741</u>		<u>51164</u>	
Structure identity (analog), %	<u>100</u> ( <u>Hyp9</u> )		<u>91.82</u> ( <u>HYP1</u> )		<u>90.24</u> ( <u>880395</u> )		<u>88.12</u> ( <u>871099</u> )	
Activity	Pa	Pi	Pa	Pi	Pa	Pi	Pa	Pi
Calcium channel (voltage-sensitive) activator	<b>0.540</b>	<b>0.052</b>	<b>0.546</b>	<b>0.048</b>	<b>0.494</b>	<b>0.083</b>	<b>0.624</b>	<b>0.017</b>
Neuropeptide Y2 antagonist	0.229	0.159	0.217	0.177	0.571	0.008	0.629	0.004
Sigma receptor agonist	0.157	0.146	0.198	0.135	0.288	0.082	0.484	0.028
Calcium channel activator	0.224	0.104	0.291	0.038	0.338	0.026	0.368	0.018
Acetylcholine neuromuscular blocking agent	--	--	0.599	0.023	0.484	0.084	0.481	0.087

Possible adverse and toxic effects

Compound number	<u>Hyp9</u>		<u>64402</u>		<u>50741</u>		<u>51164</u>	
Activity	Pa	Pi	Pa	Pi	Pa	Pi	Pa	Pi
Gastrointestinal hemorrhage	<b>0.695</b>	<b>0.026</b>	<b>0.714</b>	<b>0.021</b>	<b>0.389</b>	<b>0.157</b>	<b>0.615</b>	<b>0.050</b>

Multiple organ failure	<b>0.600</b>	<b>0.060</b>	<b>0.677</b>	<b>0.037</b>	<b>0.394</b>	<b>0.156</b>	<b>0.762</b>	<b>0.018</b>
Toxic. (v) vascular/ (r) respiration	0.798v	0.018v	0.885r	0.019r	0.096v	0.403v	0.254v	0.241v
Carcinogenic. group 1	0.306	0.055	0.357	0.033	0.115	0.401	0.200	0.161
Cardiodepressant	0.491	0.021	0.455	0.026	0.044	0.342	0.196	0.145
Carcinogenic. group 2A	0.155	0.099	0.198	0.064	0.057	0.242	0.169	0.087

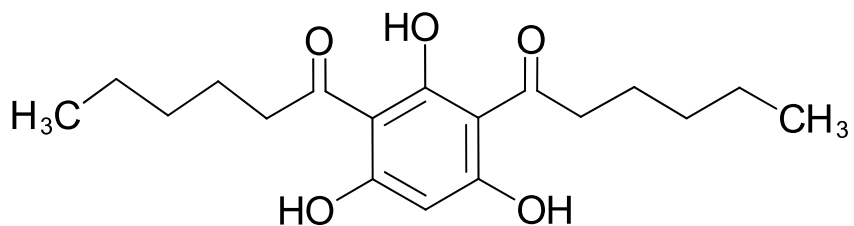
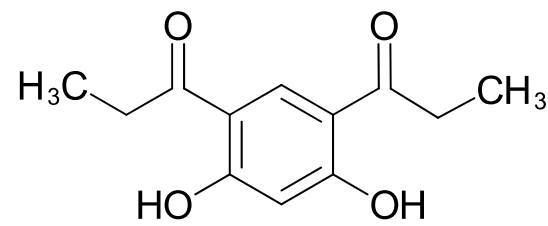
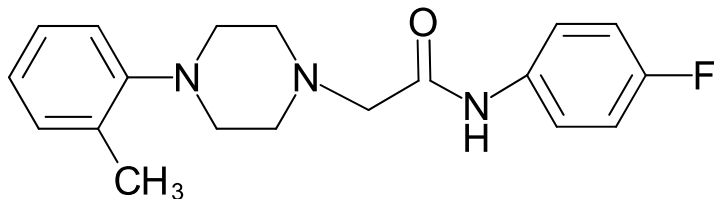
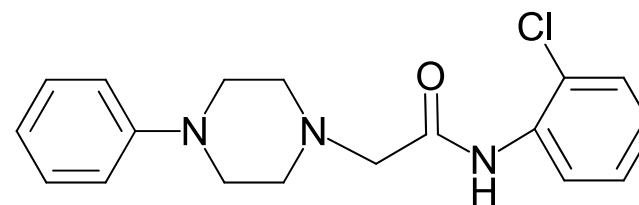
**A**Formula: C<sub>18</sub>H<sub>26</sub>O<sub>5</sub>**B**Formula: C<sub>12</sub>H<sub>14</sub>O<sub>4</sub>**C**Formula: C<sub>19</sub>H<sub>22</sub>FN<sub>3</sub>O**D**Formula: C<sub>18</sub>H<sub>20</sub>ClN<sub>3</sub>O

Fig 1

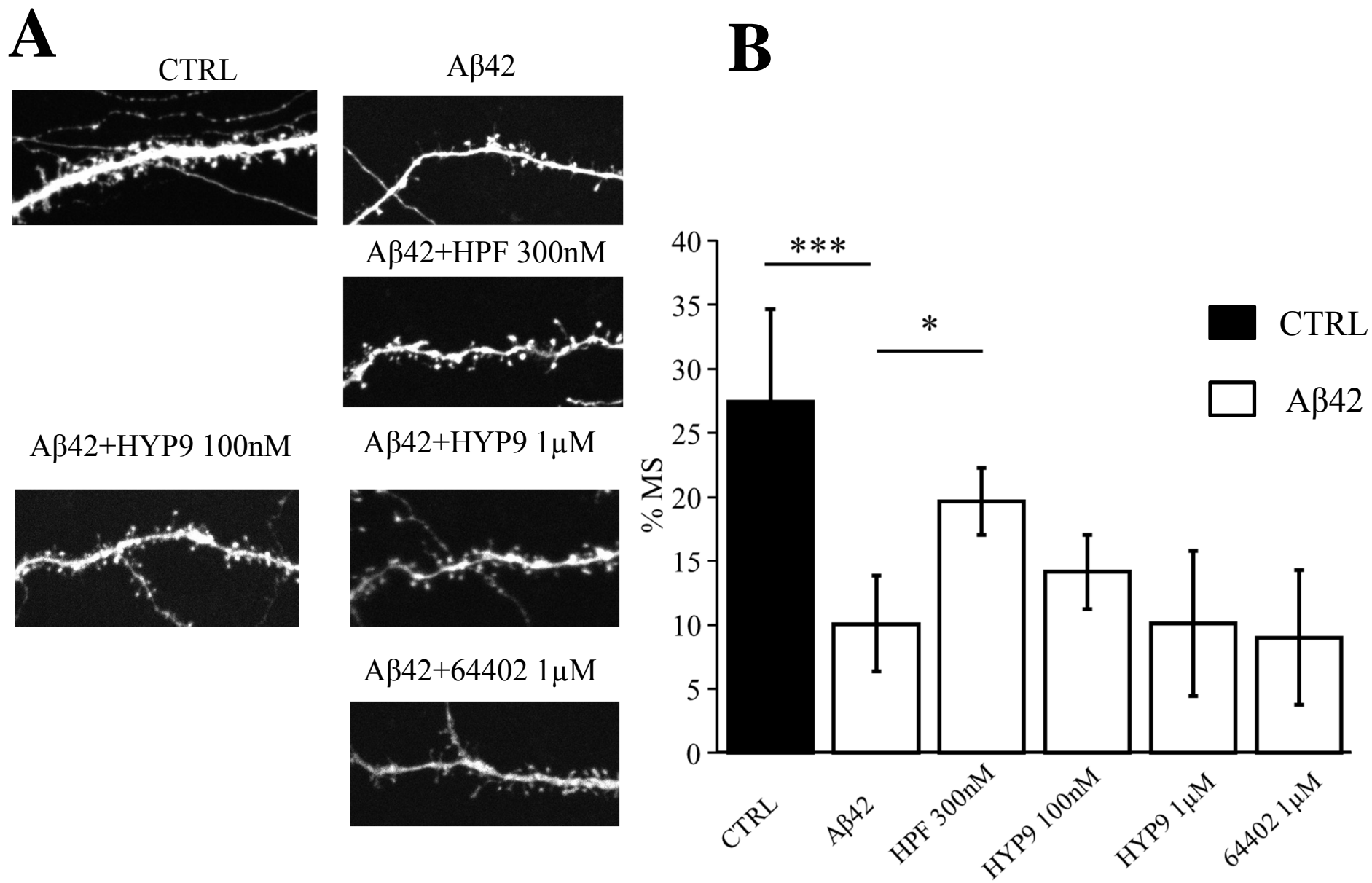
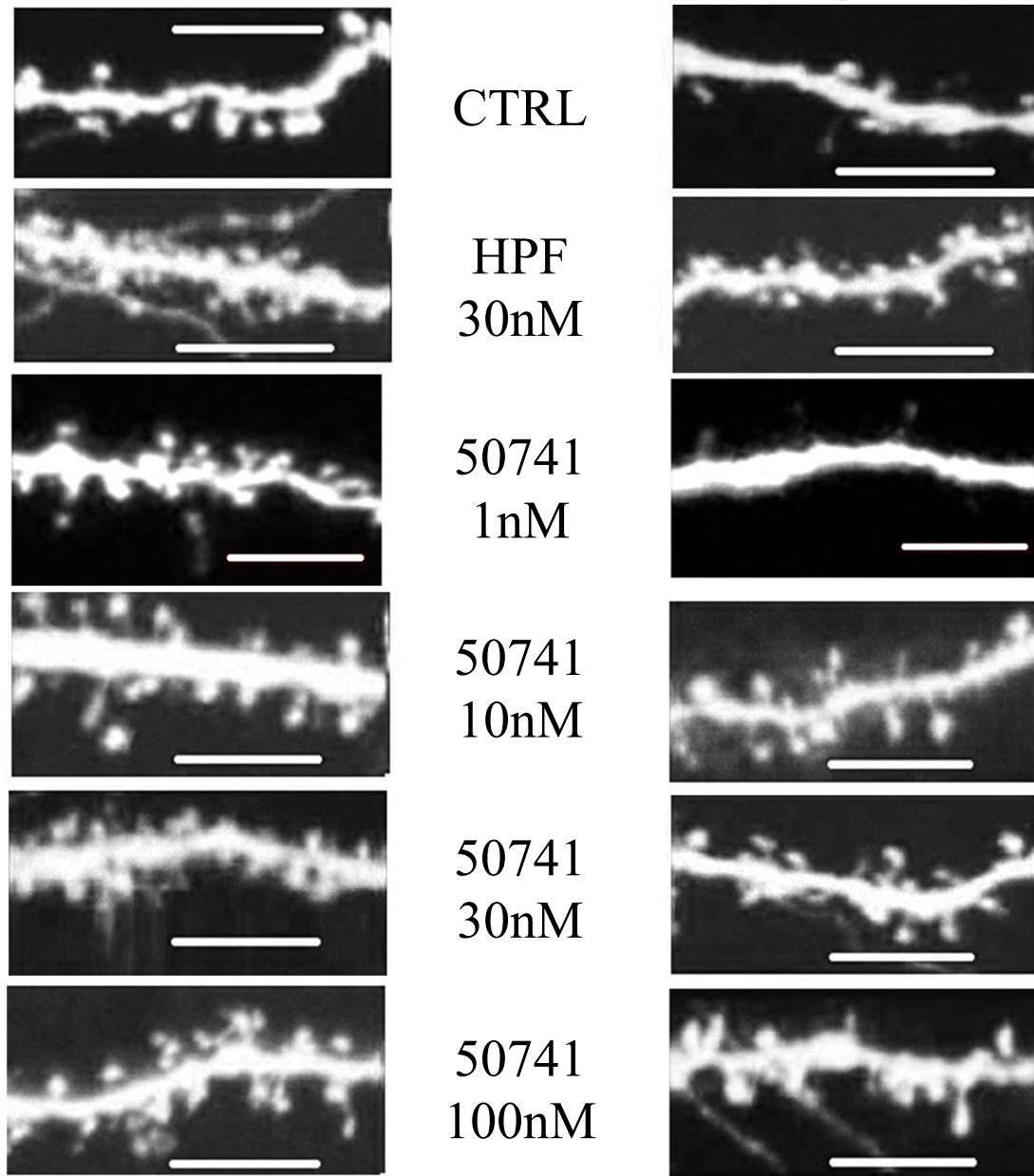


Fig 2

**A**



**B**

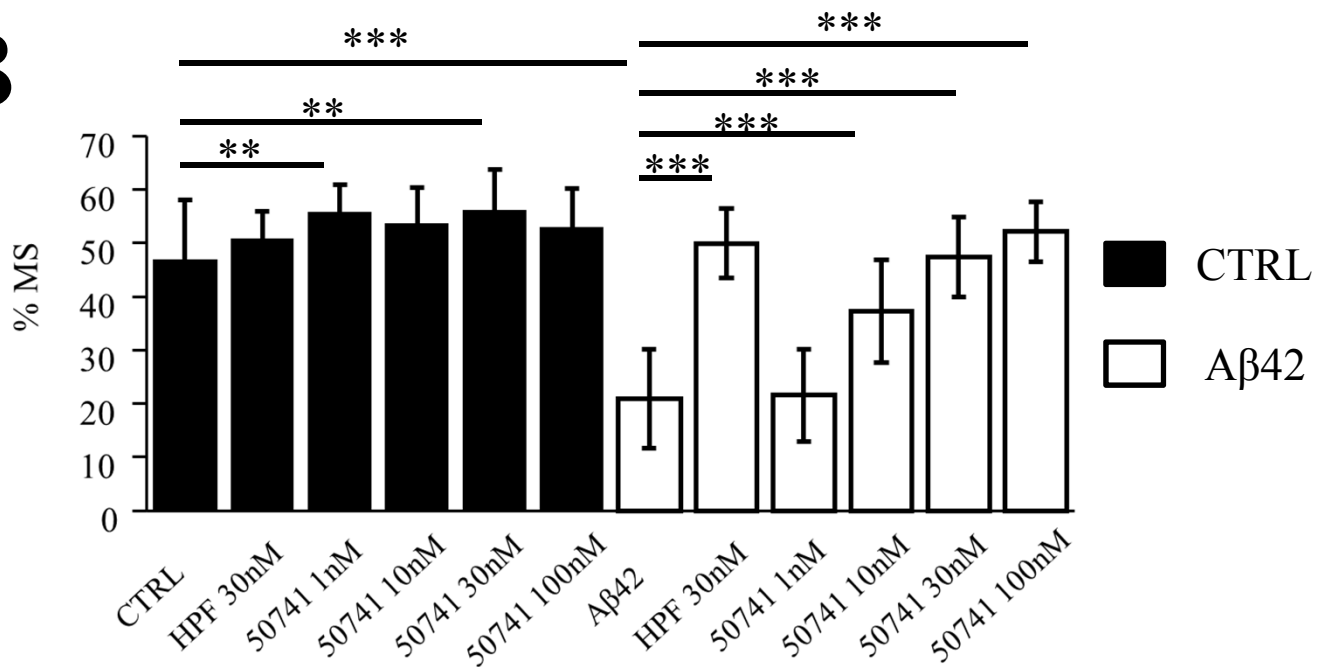


Fig 3

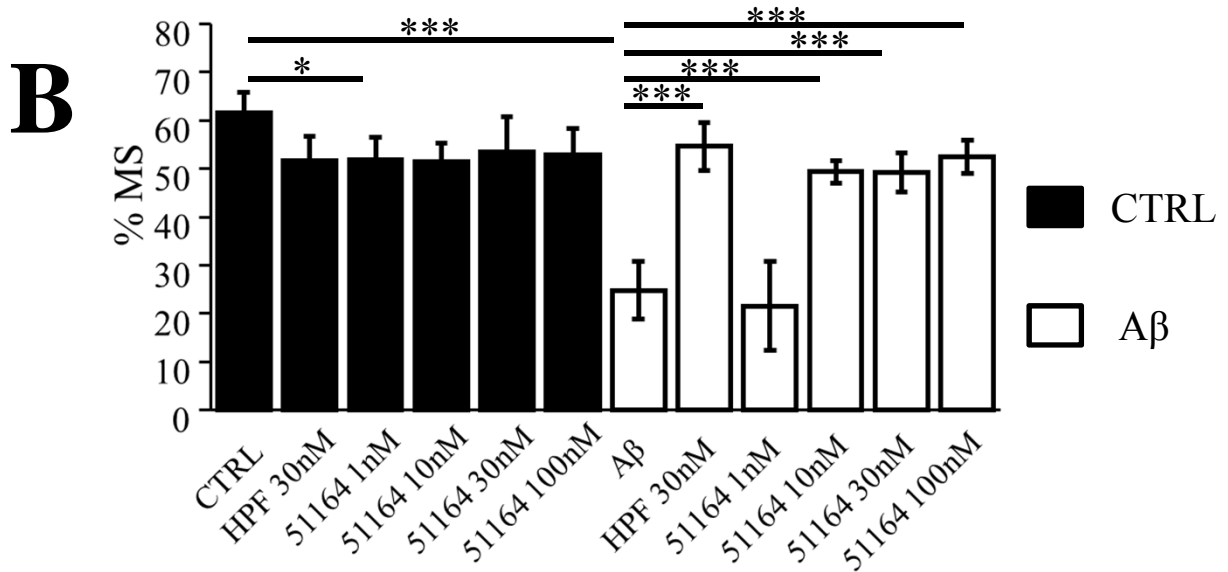
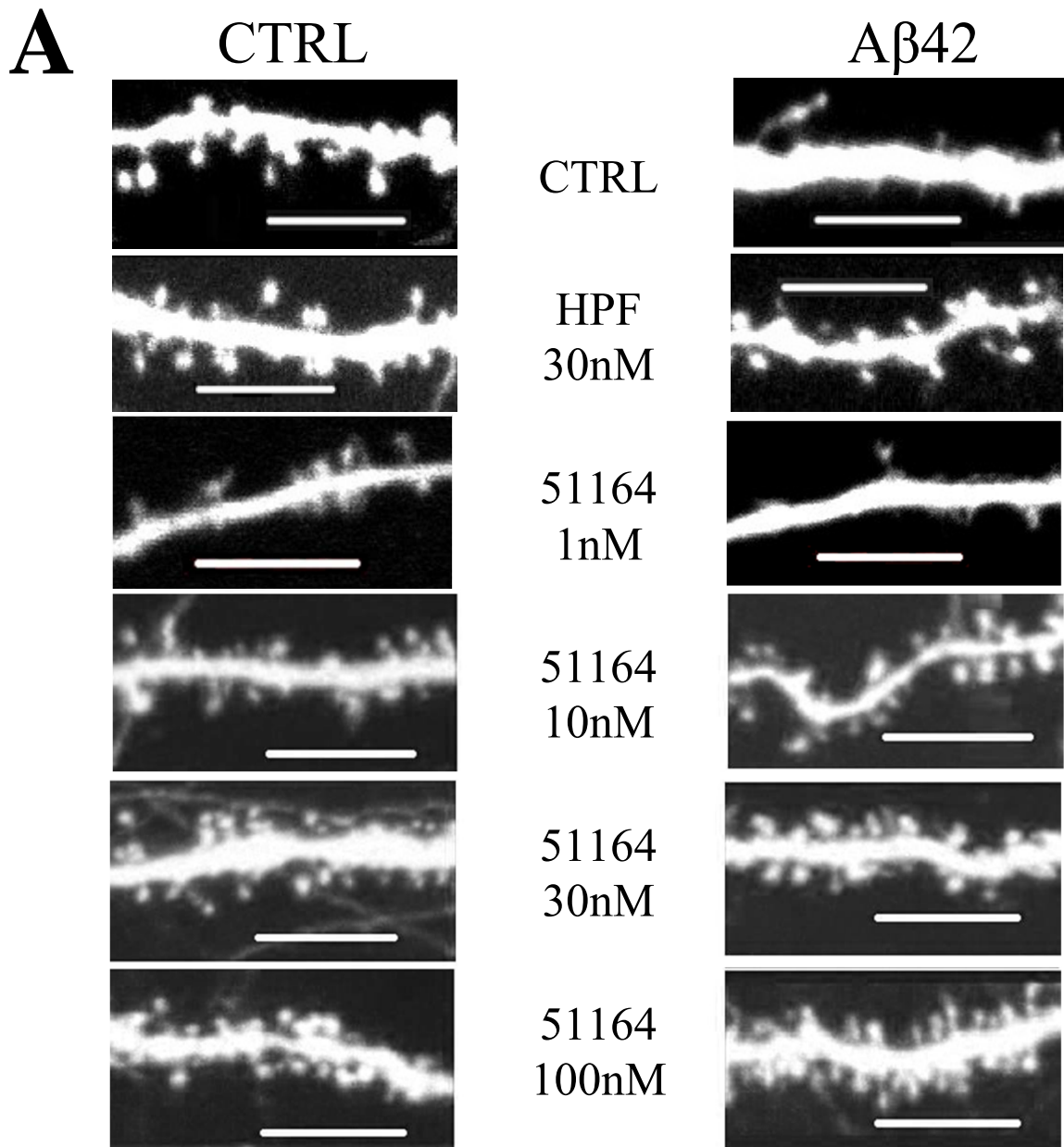


Fig 4

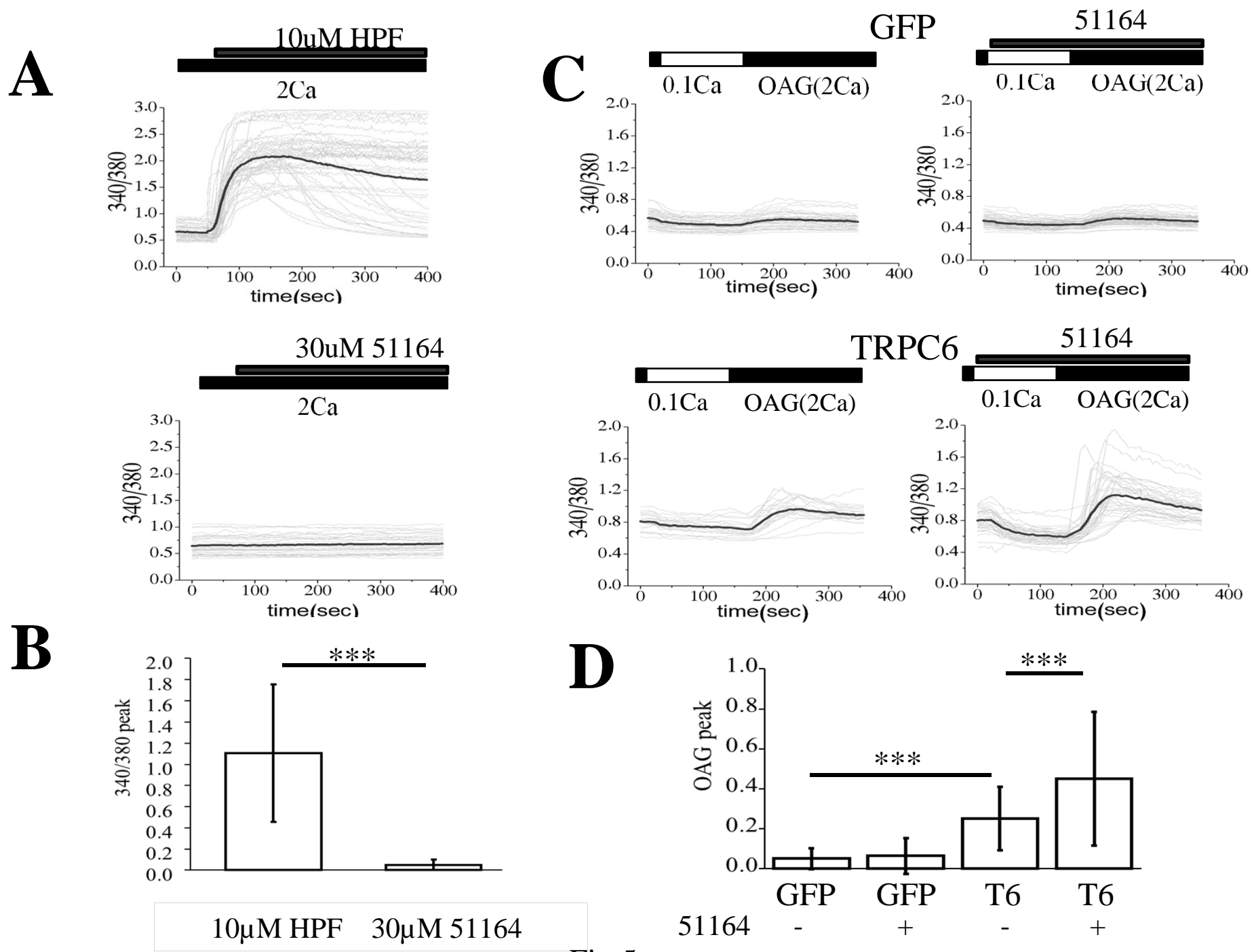


Fig 5



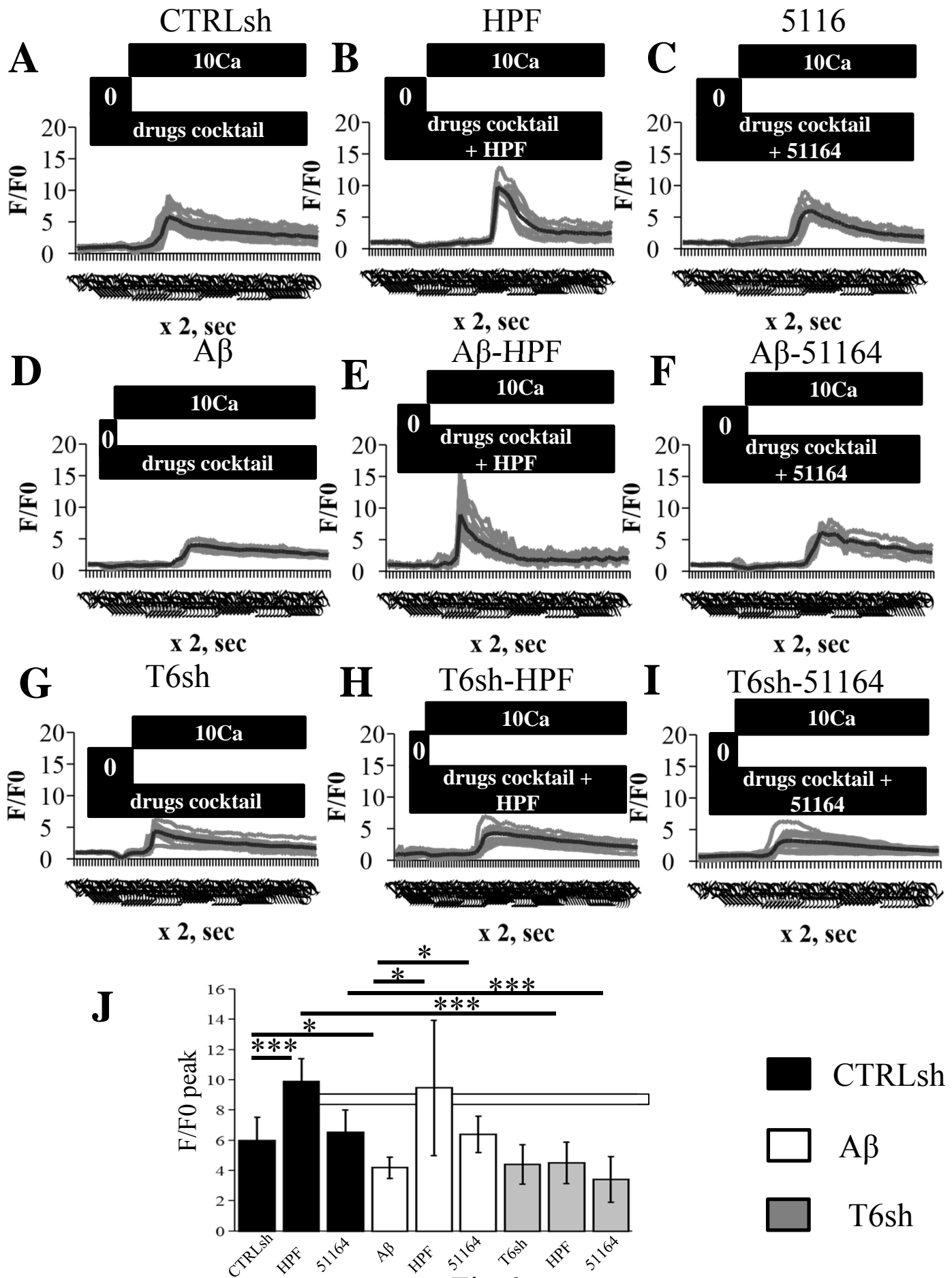


Fig 6

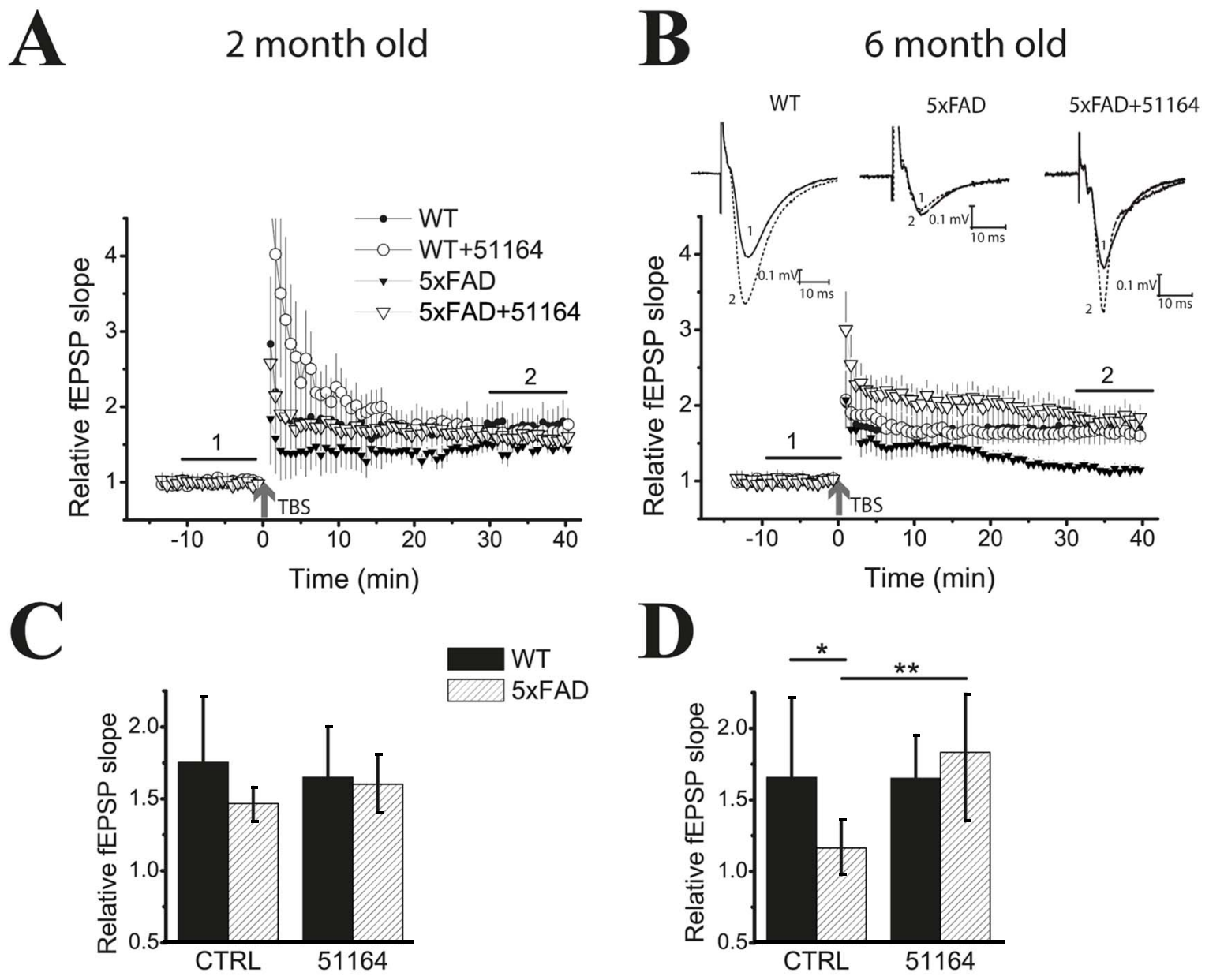


Fig 7